

Multicomponent radiatively driven stellar winds

I. Nonisothermal three-component wind of hot B stars

J. Krtička^{1,2} and J. Kubát²

¹ Katedra teoretické fyziky a astrofyziky PřF MU, Kotlářská 2, 611 37 Brno, Czech Republic

² Astronomický ústav, Akademie věd České republiky, 251 65 Ondřejov, Czech Republic

Received 12 September 2000 / Accepted 12 January 2001

Abstract. We computed models of a three-component nonisothermal radiatively driven stellar wind for different spectral types of hot B stars. We showed that friction heats mainly the outer parts of the wind and the modified temperature stratification leads to a decrease of the outflow velocity. Contrary to the isothermal case, even the possibility of decoupling of radiatively absorbing ions and (major) nonabsorbing component is excluded for a realistic form of the driving force. Regardless of the actual form of the driving force, we derived general conditions under which decoupling of a stellar wind may occur. We demonstrated that the possibility of decoupling is closely related to the functional dependence of the driving force and to the ratio of the densities of individual components. We discuss several consequences of a multifluid phenomenon in hot star winds, particularly metallicity effects and the implications of possible helium decoupling on chemically peculiar stars. We propose an explanation of the low terminal velocity of τ Sco based on frictional heating.

Key words. hydrodynamics – stars: mass-loss – stars: early-type – stars: winds – stars: individual: τ Sco

1. Introduction

In fundamental papers, Lucy & Solomon (1970) and Castor et al. (1975, hereafter CAK) showed that hot stars should have a wind driven by radiation absorbed in spectral lines. After some refinements of the theory of this wind (Abbott 1982; Friend & Abbott 1986; Pauldrach et al. 1986) it was possible to explain basic observed features of the radiatively driven stellar wind. Since the formulation of the basic theory it has been frequently assumed that the wind was isothermal to make the problem as simple as possible. Consequently, the thermal structure of the radiatively driven wind was studied only occasionally. Drew (1985) computed statistical, thermal, and ionization equilibrium of P Cygni's wind and later extended the calculations for many early-type stars (Drew 1989). She showed that energy balance of a high density wind is dominated by the equilibrium between photoionization heating and radiative cooling.

For low density winds, additional effects become important, such as the so-called Doppler heating and cooling introduced by Gayley & Owocki (1994). This effect is a natural consequence of the dependence of the radiative force on the velocity gradient (via the Doppler effect) and

physically it arises from the difference between absorption and emission frequency in the moving medium. The second mechanism is the frictional heating (Springmann & Pauldrach 1992) caused by inelastic collisions between different particles. The latter effect is also important for the overall structure of the wind, because for low-density winds, friction may not be capable of driving passive (non-absorbing) plasma. Springmann & Pauldrach proposed that the so-called “ion runaway” may occur. However, they did not solve the hydrodynamic equation itself; they mainly intended to compute temperature structure of the wind affected by frictional heating. They explained the low terminal velocity of τ Sco as a consequence of decoupling of absorbing ions.

Babel (1995) computed a three-component model of the radiatively driven wind and showed that for the case of a main-sequence A star, friction may lead to decoupling of the passive plasma. He explained the elemental separation in the atmosphere of chemically peculiar stars on the basis of the multicomponent nature of the wind. These results stimulated many authors to study the possible effects of decoupling, however, not by self-consistent solving of the appropriate hydrodynamic equations. Porter & Drew (1995) studied decoupling in the outflow from B stars, Porter & Skouza (1999) using the theory of the decoupled wind pointed out the possibility of the presence of

Send offprint requests to: J. Krtička,
e-mail: krticka@physics.muni.cz

pulsating shells around stars with low-density radiatively driven wind, and Hunger & Groote (1999) studied decoupling of helium in a stellar wind.

On the other hand, Krtićka & Kubát (2000, hereafter KK) showed on the basis of a simple theory (an isothermal two-component wind) that for late B stars friction does not lead to decoupling of the radiatively accelerated ions. They uncovered a surprising fact that friction leads to an abrupt decrease in the outflow velocity gradient. However, they pointed out that for extremely low-density winds, ion runaway may occur. The basic shortfall of this model is the isothermicity of the wind and neglecting of electrons. In this paper, we intend to include both electrons and the possible effect of the nonisothermal wind into our model.

2. Description of the model

2.1. Basic assumptions

We assume that the star has a stationary spherically symmetric radiatively driven stellar wind consisting of three ideal gas components, namely of a passive plasma (hydrogen ions with mass equal to proton mass m_p and charge equal to proton charge q_p), of absorbing ions with mass $m_i = A_i m_p$ and charge q_i , and of electrons with mass m_e and charge q_e . Finally, we assume that the temperature is the same for all three components ($T_e = T_i = T_p = T$).

2.2. Continuity and momentum equations

Each component of the wind is adequately described by the continuity equation

$$\frac{d}{dr} (r^2 \rho_a v_{ra}) = 0 \quad (1)$$

and by the equation of motion (cf. Braginskij 1963)

$$v_{ra} \frac{dv_{ra}}{dr} = g_a^{\text{rad}} - g - \frac{1}{\rho_a} \frac{dp_a}{dr} + \frac{q_a}{m_a} E + \frac{1}{\rho_a} \sum_{\substack{b=i,p,e \\ b \neq a}} R_{ab}, \quad (2)$$

where $a = i, p, e$ and subscripts i, p, e stand for metallic ions, passive plasma, and electrons, respectively. In these equations v_{ra} and ρ_a are radial velocity and density of the corresponding particles, p_a is partial pressure of each component, $p_a = a_a^2 \rho_a$ where isothermal sound speed is $a_a^2 = kT/m_a$, g is gravitational acceleration, g_a^{rad} is radiative acceleration acting on absorbing ions and electrons (we assume no radiative force acting on passive plasma), E is the charge separation electric field and R_{ab} is the frictional force exerted by component b on component a . Gravitational acceleration acting on each component of the fluid has the form $g = G\mathfrak{M}/r^2$, where \mathfrak{M} is the stellar mass and G is the gravitational constant. The radiative acceleration acting on an electron is given by the absorption on the free electrons and has the form

$$g_e^{\text{rad}} = \frac{m_p}{m_e} \frac{G\Gamma\mathfrak{M}}{r^2}, \quad (3)$$

where

$$\Gamma = \frac{\sigma_e L}{4\pi c G \mathfrak{M}}$$

is the ratio of the acting radiative force caused by absorption of radiation by free electrons and gravitational force (L is the stellar luminosity). We take the radiative acceleration acting on absorbing ions in the form (see Castor et al. 1975)

$$g_i^{\text{rad}} = \frac{1}{\mathfrak{Y}_i} \frac{\sigma_e L}{4\pi r^2 c} f \left(\frac{\rho_e / (W m_e)}{10^{11} \text{cm}^{-3}} \right)^\delta k \left(\frac{\mathfrak{Y}_i}{\sigma_e v_{\text{th}} \rho_i} \frac{dv_{ri}}{dr} \right)^\alpha, \quad (4)$$

with force multipliers k , α , δ after Abbott (1982). Here,

$$f = \frac{(1 + \sigma)^{\alpha+1} - (1 + \sigma \mu_c^2)^{\alpha+1}}{(\alpha + 1) (1 - \mu_c^2) \sigma (1 + \sigma)^\alpha}, \quad (5)$$

is the finite disk correction factor (Friend & Abbott 1986; Pauldrach et al. 1986), $v_{\text{th}} = \sqrt{2kT/m_p}$ is the thermal speed, and \mathfrak{Y}_i is the ratio of the metallic ion density to passive plasma density (we used the same value as in KK, $\mathfrak{Y}_i = 0.0127$). We introduced the latter ratio to enable calculation of the radiative force not from the whole plasma density (as is usually adopted in the standard CAK theory) but from the absorbing ion density.

There is an apparent contradiction in using the *hydrogen* thermal speed instead of the ion thermal speed. Use of the ion thermal speed seems natural, since only ions are accelerated by radiation. As was found by Abbott (1982), the acceleration from a single line in the isothermal wind is independent of the thermal speed. Therefore the choice of the formula for v_{th} is completely arbitrary, and he decided to choose the hydrogen thermal speed for the calculation of the wind parameters k , α , and δ . Since we are using his parameters for the calculation of the line force, it is necessary to use the same thermal speed for the calculation of the line force as Abbott (1982) did, namely the hydrogen thermal speed.

Frictional force (per unit volume) R_{ab} acting between both components has the form (Springmann & Pauldrach 1992):

$$R_{ab} = -n_a n_b k_{ab} G(x_{ab}). \quad (6)$$

The friction coefficient k_{ab} is given by

$$k_{ab} = \frac{4\pi \ln \Lambda q_a^2 q_b^2}{kT} \frac{v_{ra} - v_{rb}}{|v_{ra} - v_{rb}|}. \quad (7)$$

The Coulomb logarithm is of the form (cf. Lang 1974)

$$\ln \Lambda = \ln \left[\frac{24\pi}{\sqrt{n}} \left(\frac{kT}{4\pi e^2} \right)^{3/2} \right], \quad (8)$$

where n is the particle density ($n = n_p + n_e + n_i$), e is the elementary charge, $G(x)$ is so the called Chandrasekhar function, which is defined in terms of the error function $\Phi(x)$ (see Dreicer 1959)

$$G(x) = \frac{1}{2x^2} \left(\Phi(x) - x \frac{d\Phi(x)}{dx} \right). \quad (9)$$

The Chandrasekhar function has the following behavior. For $x \ll 1$ is $G(x) \sim x$, for $x \approx 1$ reaches its maximum value and for $x \gg 1$ is $G(x) \sim x^{-2}$. The argument of the Chandrasekhar function in Eq. (6) is

$$x_{ab} = \sqrt{A_{ab}} \frac{|v_{ra} - v_{rb}|}{v_{th}}, \quad (10)$$

where $A_{ab} = A_a A_b / (A_a + A_b)$ is the reduced atomic mass.

The term $v_{re} dv_{re} / dr$ in the electron momentum equation can be neglected compared to the electron pressure term and consequently the electron momentum equation can be used to determine charge separation electric field E

$$\frac{e}{m_e} E = g_e^{\text{rad}} - g + \frac{1}{\rho_e} (R_{ep} + R_{ei}) - \frac{1}{\rho_e} \frac{dp_e}{dr}. \quad (11)$$

Electron velocity and density are calculated from the condition of quasi-neutrality and from the zero current condition

$$n_e = n_p + z_i n_i \quad (12)$$

$$n_e v_{re} = n_p v_{rp} + z_i n_i v_{ri}. \quad (13)$$

2.3. Energy equation

We assume a nonisothermal wind, so the system of continuity and momentum equations should be supplemented by the energy (heat transfer) equation which in the case of equal temperature of all components takes the form

$$\begin{aligned} \sum_{a=p,e,i} \frac{1}{r^2} \frac{d}{dr} (r^2 u_a v_{ra}) + \sum_{a=p,e,i} a_a^2 \rho_a \frac{1}{r^2} \frac{d}{dr} (r^2 v_{ra}) \\ = Q^{\text{rad}} - \frac{1}{2} \sum_{a=p,e,i} \sum_{\substack{b=p,e,i \\ b \neq a}} R_{ab} (v_{ra} - v_{rb}). \end{aligned} \quad (14)$$

The internal energy is chosen to be $u_a = 3/2 n_a kT$. Apparently, using continuity Eq. (1) the heat transfer equation can be rewritten in a more simple form

$$\begin{aligned} \frac{3}{2} k \frac{dT}{dr} \sum_{a=p,e,i} v_{ra} \frac{\rho_a}{m_a} + \sum_{a=p,e,i} a_a^2 \rho_a \frac{1}{r^2} \frac{d}{dr} (r^2 v_{ra}) \\ = Q^{\text{rad}} - \frac{1}{2} \sum_{a=p,e,i} \sum_{\substack{b=p,e,i \\ b \neq a}} R_{ab} (v_{ra} - v_{rb}). \end{aligned} \quad (15)$$

Two terms on the left-hand side describe advection and adiabatic cooling, respectively. The right-hand side terms stand for radiative heating/cooling and for frictional heating, respectively.

2.3.1. Radiative energy term

For consistent determination of radiative heating and cooling it would be necessary to include all bound-free and free-free transitions for all species considered and also inelastic collisions, and to solve a complete set of equations

of statistical equilibrium as well as the radiative transfer equation. It would be computationally very costly.

The main sources of radiative heating and cooling in the atmospheres of hot stars are the hydrogen Lyman bound-free and free-free transitions. According to NLTE hydrogen-helium model atmosphere calculations (Kubát 2001) the contribution of inelastic collisions to heating/cooling is much smaller in the outermost parts of the atmosphere (at least by a factor of 100). Note that radiative bound-bound transitions do not contribute to the radiative heating/cooling term Q^{rad} , since they transfer energy between radiation and internal energy of atoms and the amount of energy transferred directly to the ionic motion is negligible. Thus, we decided to estimate the radiative heating/cooling term Q^{rad} using the former two mechanisms only (hydrogen Lyman bound-free and free-free transitions). The detailed form of heating and cooling in the above-mentioned transitions is (see Kubát et al. 1999)

$$Q_{\text{ff}}^{\text{H}} = 4\pi n_e N_{\text{H}^+} \int_0^\infty \alpha_{\text{ff}}(\nu, T) J_\nu d\nu, \quad (16a)$$

$$Q_{\text{ff}}^{\text{C}} = 4\pi n_e N_{\text{H}^+} \int_0^\infty \alpha_{\text{ff}}(\nu, T) \left(J_\nu + \frac{2h\nu^3}{c^2} \right) \times e^{-h\nu/kT} d\nu, \quad (16b)$$

$$Q_{\text{bf}}^{\text{H}} = 4\pi \sum_l n_l \int_0^\infty \alpha_{\text{bf},l}(\nu) J_\nu \left(1 - \frac{\nu_l}{\nu} \right) d\nu, \quad (16c)$$

$$Q_{\text{bf}}^{\text{C}} = 4\pi \sum_l n_l \int_0^\infty \alpha_{\text{bf},l}(\nu) \left(J_\nu + \frac{2h\nu^3}{c^2} \right) \times e^{-h\nu/kT} \left(1 - \frac{\nu_l}{\nu} \right) d\nu, \quad (16d)$$

and the total energy transferred via radiation is

$$Q^{\text{rad}} = Q_{\text{ff}}^{\text{H}} + Q_{\text{bf}}^{\text{H}} - Q_{\text{ff}}^{\text{C}} - Q_{\text{bf}}^{\text{C}}. \quad (17)$$

Free-free and photoionization cross-sections are taken from Mihalas (1978), J_ν is considered to be constant throughout the wind and it is taken as emergent radiation from a spherically symmetric static hydrogen model atmosphere for a corresponding stellar type (Kubát 2001).

2.4. Critical points

Generally, critical points are points where derivatives of individual variables cannot be determined directly from equations. A three-component stellar wind generally should have three critical points. However, neglecting the term containing the derivative of the electron velocity in the electron equation of motion simplifies the problem, leaving only two critical points.

Below we write the equations of motion and energy in a simplified form. We include all terms without derivatives into the terms F_i ($i = a$ for the equations of motion, $i = 3$

for the energy equation). The equations of motion then read

$$v_{ra} \frac{dv_{ra}}{dr} = - \frac{a_a^2}{n_a} \frac{dn_a}{dr} - \frac{da_a^2}{dr} - z_a \frac{a_a^2}{n_e} \frac{dn_e}{dr} - z_a \frac{da_a^2}{dr} + g_a^{\text{rad}} + F_a(r, v_{ra}, n_a, v_{rb}, n_b, T), \quad (18)$$

where $z_a = q_a/e$. Similarly, the energy equation can be rewritten as

$$-\frac{1}{T} \frac{dT}{dr} = \frac{2}{3} \frac{\sum_b n_b \frac{dv_{rb}}{dr}}{\sum_b n_b v_{rb}} + F_3(v_{ra}, n_a, v_{rb}, n_b, T). \quad (19)$$

Expressing derivatives of temperature, densities of each component and electron velocity with the help of derivatives of passive plasma and the velocity of absorbing ions, we arrive at a matrix form of the equations, namely

$$D \cdot \mathbf{y} = \mathbf{b}, \quad (20)$$

where \mathbf{y} is the column vector, defined as

$$\mathbf{y} = \begin{pmatrix} \frac{1}{v_{rp}} \frac{dv_{rp}}{dr} \\ \frac{1}{v_{ri}} \frac{dv_{ri}}{dr} \end{pmatrix}. \quad (21)$$

The column vector \mathbf{b} does not depend on any of the derivatives and includes the terms F_i from Eqs. (18) and (19). Diagonal elements of the matrix D are

$$D_{aa} = v_{ra}^2 - v_{ra} \frac{\partial g_a^{\text{rad}}}{\partial (dv_{ra}/dr)} - a_a^2 \left[1 + \frac{n_a}{n_e} \left(z_a^2 + \frac{2}{3} (1 + z_a) \frac{n_e (v_{ra} + z_a v_{re})}{\sum_{b \neq e} (1 + z_b) n_b v_{rb}} \right) \right] \quad (22)$$

where a stands for i or p, and off-diagonal elements read

$$D_{ac} = -a_a^2 \frac{n_c}{n_e} \left[z_c z_a + \frac{2}{3} (1 + z_a) \frac{n_e (v_{rc} + z_c v_{re})}{\sum_{b \neq e} (1 + z_b) n_b v_{rb}} \right], \quad (23)$$

where a, c stands for i or p. In these equations we accounted for quasineutrality and zero-current conditions (Eqs. (12), (13)).

At singular points, the determinant of matrix D equals zero. General calculation of singular points for arbitrary values of number densities would be rather complicated. One should look for two roots of an equation

$$D_{pp} D_{ii} - D_{pi} D_{ip} = 0. \quad (24)$$

Thus, we confine our discussion to a realistic case, when the ionic number density is much lower than the passive plasma number density. In this case, the off-diagonal terms

D_{pi} can be neglected, and Eq. (24) can be split into two equations that determine the critical points, namely

$$D_{pp} = 0 \quad (25a)$$

$$D_{ii} = 0. \quad (25b)$$

Note that such separation of two critical points is possible not only in the standard case $n_i \ll n_p$, but also in the nonrealistic case, $n_i \gg n_p$.

However, when the wind is not decoupled (i.e. $v_{ri} \approx v_{rp}$), the second condition (25b) is not met anywhere in the wind, because the non-zero term containing the derivative of the radiative force is substantially higher than the other terms (see also KK). Therefore, different condition must be used to fix the mass-loss rate.

Such condition can be derived from momentum equations (2) by multiplying the equations for absorbing ions and passive plasma by the corresponding density and summing them (again, only terms including derivatives of variables are explicitly written, the rest is included in the term F_i), namely

$$\rho_p \left(v_{rp} - \frac{a_p^2}{v_{rp}} \right) \frac{dv_{rp}}{dr} + \rho_i \left(v_{ri} - \frac{a_i^2}{v_{ri}} \right) \frac{dv_{ri}}{dr} - \rho_i g_i^{\text{rad}} + \frac{1}{T} (\rho_p a_p^2 + \rho_i a_i^2) \frac{dT}{dr} + \frac{\rho_p}{\rho_e} \frac{d(a_p^2 \rho_e)}{dr} + z_i \frac{\rho_i}{\rho_e} \frac{d(a_i^2 \rho_e)}{dr} = F_4(r, \rho_a, v_{ra}, T). \quad (26)$$

Using the quasineutrality Eq. (12) and recalling Eq. (19), we obtain

$$\rho_p \left(v_{rp} - \frac{a_p^2}{v_{rp}} \right) \frac{dv_{rp}}{dr} + \rho_i \left(v_{ri} - \frac{a_i^2}{v_{ri}} \right) \frac{dv_{ri}}{dr} - \rho_i g_i^{\text{rad}} + \frac{1}{T} (2\rho_p a_p^2 + (1 + z_i) \rho_i a_i^2) \frac{dT}{dr} - \left(a_p^2 \frac{\rho_p}{\rho_e} + z_i a_i^2 \frac{\rho_i}{\rho_e} \right) \left(\frac{m_e}{m_p} \frac{\rho_p}{v_{rp}} \frac{dv_{rp}}{dr} + z_i \frac{m_e}{m_i} \frac{\rho_i}{v_{ri}} \frac{dv_{ri}}{dr} \right) = F_5(r, \rho_a, v_{ra}, T). \quad (27)$$

Finally, if the condition

$$\rho_p \left(v_{rp} - \frac{a_p^2}{v_{rp}} \right) \frac{dv_{rp}}{dr} + \rho_i \left(v_{ri} - \frac{a_i^2}{v_{ri}} - \frac{\partial g_i^{\text{rad}}}{\partial (dv_{ri}/dr)} \right) \frac{dv_{ri}}{dr} + \frac{1}{T} (2\rho_p a_p^2 + (1 + z_i) \rho_i a_i^2) \frac{dT}{dr} - \left(a_p^2 \frac{\rho_p}{\rho_e} + z_i a_i^2 \frac{\rho_i}{\rho_e} \right) \times \left(\frac{m_e}{m_p} \frac{\rho_p}{v_{rp}} \frac{dv_{rp}}{dr} + z_i \frac{m_e}{m_i} \frac{\rho_i}{v_{ri}} \frac{dv_{ri}}{dr} \right) = 0 \quad (28)$$

holds, then the total equation of motion (26) does not depend on the derivatives of any variables. This condition is used to fix the mass-loss rate (see Sect. 2.6).

The fact that the ionic critical point is not met anywhere in the wind is very interesting, particularly in connection with the so-called Abbott waves (Abbott 1980). At first glance, one can conclude that such *purely ionic* Abbott waves can disseminate from any point in the wind upstream of the flow. However, our preliminary simple

linear stability analysis of the two-component case indicates that such purely ionic Abbott waves are heavily damped when the corresponding Chandrasekhar function does not reach its maximum value. Thus, similar to the one-component case, the last point in the wind from which upstream waves can propagate is that defined by Eq. (28). The detailed stability analysis will be presented in our next paper.

2.5. Boundary conditions

2.5.1. Boundary condition for temperature

We assume that at the inner boundary, radiative equilibrium holds, therefore the boundary condition for temperature is

$$Q^{\text{rad}}(R_*) = 0. \quad (29)$$

2.5.2. Boundary condition for velocity

To avoid problems concerning two critical points, we start to calculate our models at the passive plasma critical point; consequently, the boundary condition for passive plasma velocity is (see Eq. (22), (25a))

$$v_{r_p}^2(R_*) = a_p^2 \left[1 + \frac{n_p}{n_e} \left(z_p^2 + \frac{2}{3} (1 + z_p) \frac{n_e (v_{r_p} + z_p v_{r_e})}{\sum_{b \neq e} (1 + z_b) n_b v_{r_b}} \right) \right]. \quad (30)$$

The boundary condition for absorbing ions can be derived from the passive plasma equation of motion (2), which at the passive plasma critical point may be rewritten as

$$\begin{aligned} \frac{R_{p_i}}{\rho_p} + \left(1 - \frac{n_p}{n_e} \right) \frac{R_{p_e}}{\rho_p} + \frac{m_e}{m_p} \frac{R_{e_i}}{\rho_e} \\ = \frac{G\mathfrak{M}}{r^2} \left(1 - \Gamma + \frac{m_e}{m_p} \right) - \frac{4a_p^2}{r}, \end{aligned} \quad (31)$$

where we used the boundary condition for temperature (29) and neglected frictional heating. For stars with solar abundances, we may further neglect the number density of absorbing ions, ($n_e \gg n_i$), and taking into account that the electron and passive plasma number densities are nearly equal ($n_p \approx n_e$) we write the boundary condition for absorbing ions in a simpler form,

$$\frac{R_{p_i}}{\rho_p} + \frac{m_e}{m_p} \frac{R_{e_i}}{\rho_e} = -\frac{4a_p^2}{r} + \frac{G\mathfrak{M}}{r^2} (1 - \Gamma), \quad (32)$$

which was used in our models.

Further simplification of the boundary condition for ion velocity may be obtained by taking into account the fact that the individual components are fully coupled at the base of the wind, as is the case in our models. The boundary condition then takes the much simpler form

$$v_{r_p}(R_*) = v_{r_i}(R_*). \quad (33)$$

Thus, our results do not change significantly if we suppose that velocities of all components are equal at the base of the wind. We incorporated the possibility of different boundary velocities only for the sake of physical consistence of our models.

2.5.3. Boundary condition for density

Providing that at some point deep in the atmosphere (with radius $r_{\text{at}} < R_*$), both passive plasma and absorbing ion velocities are nearly equal, then

$$\rho_i(r_{\text{at}}) = \mathfrak{Y}_i \rho_p(r_{\text{at}}). \quad (34)$$

Finally, using the continuity Eq. (1), the boundary condition for the passive plasma density may be written in the form

$$\rho_p(R_*) = \frac{1}{\mathfrak{Y}_i} \rho_i(R_*) \frac{v_{r_i}(R_*)}{v_{r_p}(R_*)}. \quad (35)$$

The boundary value of ionic density is chosen in order to obtain the three-component CAK solution (see Sect. 2.6).

2.5.4. Boundary conditions for electrons

The charge conservation Eq. (12) and zero current condition (13) can be used directly as boundary conditions for electron density and electron velocity, respectively.

2.6. Numerical method

There exist several numerical methods that may be suitable for this problem. As an example, methods based on numerical simulations are frequently applied. The system is simply allowed to develop until it reaches a stationary state. Such a method was used for the investigation of stellar wind structure, particularly in 2D, e.g. by Owocki et al. (1994) and Petrenz & Puls (2000). Another method (integral method) was developed by Beutler (1979) and was applied to a solar wind problem by Bürgi (1992).

The Henyey method (Henyey et al. 1964) was used to solve equations of the radiatively driven stellar wind by Nobili & Turolla (1988). This method a modified Newton-Raphson method. The hydrodynamic equations are linearized and also the CAK condition is included into the set of linearized equations. The latter method was selected by us.

Equations, which we solve (i.e. Eqs. (1), (2), (12), (13), (15)) together with the appropriate boundary conditions (Eqs. (12), (13), (29), (32), (35)) may formally be written as

$$\mathbf{P}\psi = 0, \quad (36)$$

where ψ is a column vector of variables (NR is the number of grid points),

$$\begin{aligned} \psi = (\rho_{i1}, v_{r_{i1}}, \rho_{p1}, v_{r_{p1}}, \rho_{e1}, v_{r_{e1}}, T_1, \\ \rho_{i2}, v_{r_{i2}}, \rho_{p2}, v_{r_{p2}}, \rho_{e2}, v_{r_{e2}}, T_2, \dots, \\ \rho_{i\text{NR}}, v_{r_{i\text{NR}}}, \rho_{p\text{NR}}, v_{r_{p\text{NR}}}, \rho_{e\text{NR}}, v_{r_{e\text{NR}}}, T_{\text{NR}}) \end{aligned} \quad (37)$$

and \mathbf{P} is a non-linear operator. The Newton-Raphson method adopted here employs the iterative scheme

$$\hat{J}^n \delta\psi^{n+1} = -\mathbf{P}^n \psi^n, \quad (38)$$

where ψ^n is solution in the n th iteration and \hat{J}^n is the Jacobian in the n th iteration,

$$\hat{J}_{kl}^n = \frac{\partial P_k}{\partial \psi_l}. \quad (39)$$

To solve the system of Eqs. (38) for $\delta\psi^{n+1}$ we used the numerical package LAPACK, developed at the University of Tennessee.

Although the original Henyey method handles critical points well (Nobili & Turolla 1988), due to some numerical problems we decided to modify the method as described in KK. Here we only briefly summarize our approach. For each model we search for the boundary density $\rho_0 = \rho_p(R_*)$ that enables us to pass smoothly through the point similar to the CAK point defined by the Eq. (28). In each step we fix the value of ρ_0 , perform several Newton-Raphson iterations (described above) and after inspection of the obtained results we modify its value in the following manner. If condition (28) is not met, we increase the value of ρ_0 , whereas in the opposite case (or even if the model does not converge) we decrease the value of ρ_0 . The steps are repeated until a satisfactory value of ρ_0 is obtained (i.e. the error of our estimate of ρ_0 is 1%). Note that this a bit complicated procedure affects only the resulting mass-loss rate and does not change the overall picture of the downstream flow.

2.7. One-component models

For comparison purposes, we also calculated one-component models of a stellar wind. They are described by continuity Eq. (1), equation of motion (2), and energy Eq. (15), where ρ_a and v_{ra} are replaced by density and velocity of the whole fluid ρ , v_r , respectively. Friction terms and electric charge separation electric field are not accounted for. The one-component equations are

$$\frac{d}{dr} (r^2 \rho v_r) = 0 \quad (40a)$$

$$v_r \frac{dv_r}{dr} - g^{\text{rad}} + g + \frac{2}{\rho} \frac{d(a_p^2 \rho)}{dr} = 0 \quad (40b)$$

$$3k \frac{dT}{dr} v_r \frac{\rho}{m_p} + 2a_p^2 \rho \frac{1}{r^2} \frac{d}{dr} (r^2 v_r) - Q^{\text{rad}} = 0, \quad (40c)$$

where the radiative force is (compared to three-component notation)

$$g^{\text{rad}} \left(r, \rho, v_r, \frac{dv_r}{dr} \right) = \mathfrak{Y}_i g_i^{\text{rad}} \left(r, \mathfrak{Y}_i^{-1} \rho_i, v_{r_i}, \frac{dv_{r_i}}{dr} \right).$$

Inserting derivatives of density (from continuity Eq. (40a) and temperature (from energy Eq. (40c)) into the equation of motion (40b) we obtain the critical point of the above

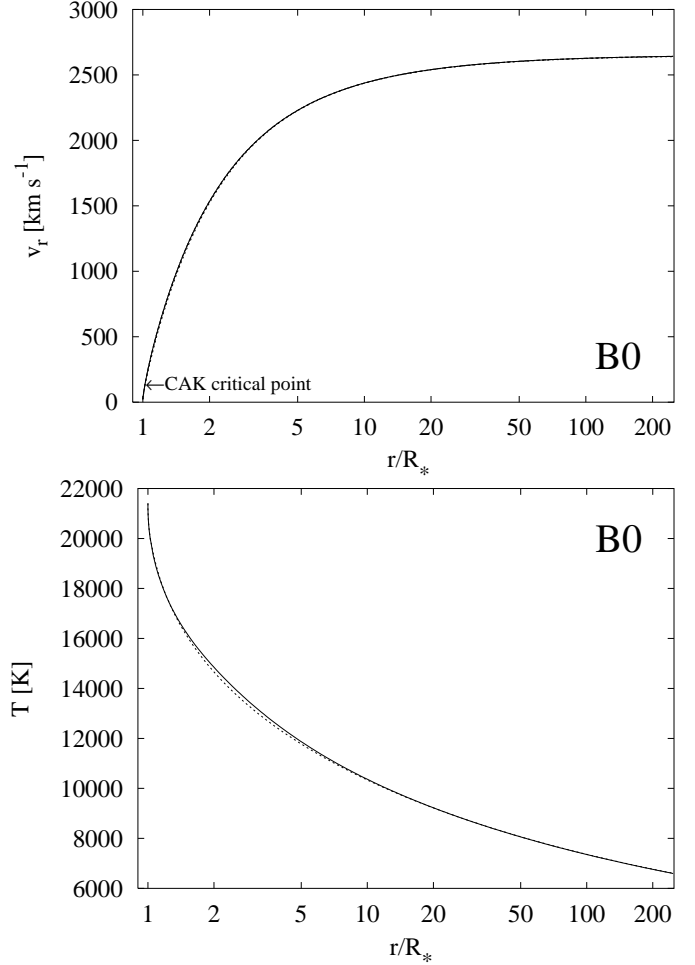


Fig. 1. *Upper panel:* one-component (dotted line) and three-component (radiatively accelerated ions – dashed line, passive plasma and electrons – full line) radiatively driven stellar wind model of a B0 star. Notice that both curves coincide. In addition, the location of the CAK critical point for both wind models is almost the same and it is given by condition (28). *Lower panel:* comparison of temperature stratification of one-component (dotted line) and three-component (solid line) radiatively driven stellar wind models of a B0 star

system of equations (the well known CAK critical point) in the form

$$v_r - \frac{10 a_p^2}{3 v_r} - \frac{\partial g^{\text{rad}}}{\partial (dv_r/dr)} = 0. \quad (41)$$

To solve this set of equations, we used the same method as described in Sect. 2.6, however, with essentially lower number of variables and equations.

3. Results of calculations

Parameters of model stars are given in Table 1. Main sequence stellar parameters are taken from Harmanec (1988) and force multipliers are adopted from Abbott (1982).

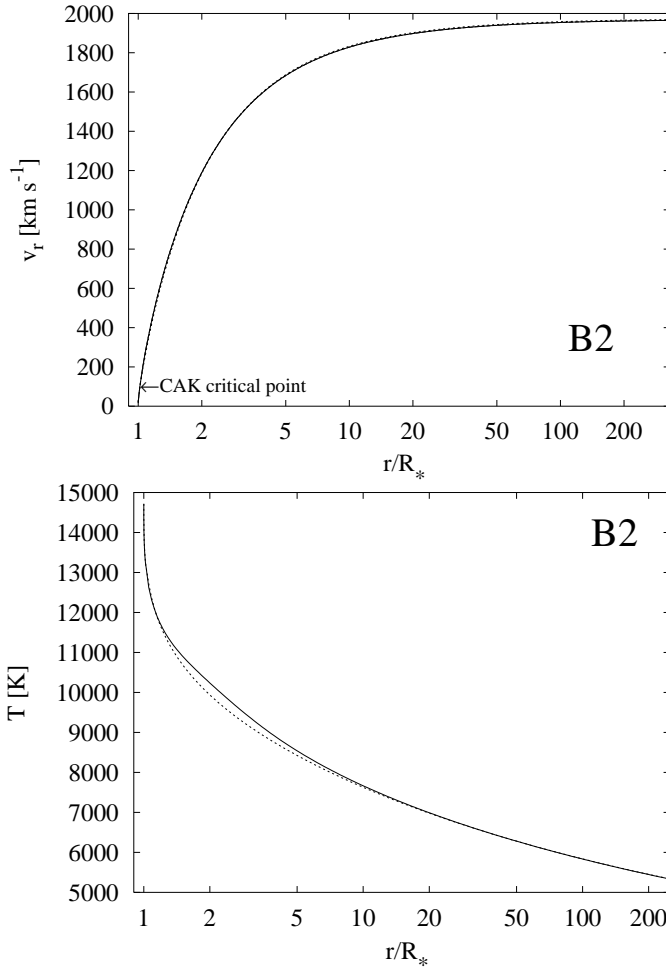


Fig. 2. The same as Fig. 1 for a B2 star

Table 1. *Adopted parameters of model stars.* \mathfrak{M} is the stellar mass in units of solar mass, R_* is the stellar radius in units of solar radius, T_{eff} is the star’s effective temperature, k , α , and δ are radiative force multipliers, q_i/q_p is the ionic charge and A_i is the atomic number of a radiatively driven ion

Stellar type (star)	Stellar parameters			Wind parameters			Average ion	
	\mathfrak{M} [\mathfrak{M}_\odot]	R_* [R_\odot]	T_{eff} [K]	k	α	δ	A_i	q_i/q_p
B0	14.57	5.80	29 900	0.156	0.609	0.120	12.0	2.0
B1	11.03	4.91	26 200	0.278	0.570	0.100	12.0	2.0
B2	8.62	4.28	23 100	0.377	0.537	0.091	12.0	2.0
B3	6.07	3.56	19 100	0.477	0.506	0.089	12.0	2.0
B4	5.12	3.26	17 200	0.365	0.509	0.105	12.0	2.0
B5	4.36	3.01	15 500	0.235	0.511	0.12	12.0	2.0
τ Sco	18.00	6.22	32 000	0.113	0.604	0.095	12.0	2.0

3.1. Stellar winds with no significant effect of friction

For stars with high density winds where the drift velocity between components is low compared to the thermal speed, no significant differences between one-component and three-component winds occur. This behavior is shown in Figs. 1 and 2 for the case of B0 and B2 stars, respectively. The temperature profile of such wind is controlled

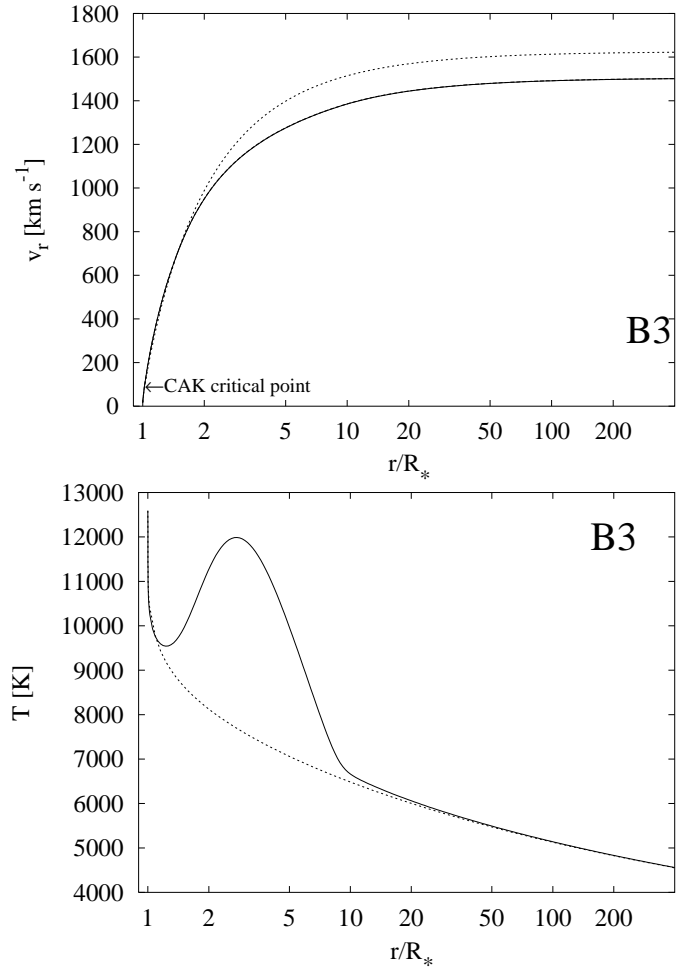


Fig. 3. The same as Fig. 1 for a B3 star. Notice the differences both in velocities and in temperature structure caused by frictional heating (see the text)

mainly by equilibrium between radiative heating and radiative cooling.

Similar models have been previously described by other authors (Springmann & Pauldrach 1992, model of ζ Pup therein, KK, model of ϵ Ori therein), however, using simpler assumptions.

3.2. Decrease of the outflow velocity due to frictional heating

For stars with lower density, friction begins to play an important role (see Figs. 3 and 5 for the case of B3 and B4 stars, respectively). To maintain the common flow, a sufficient amount of momentum must be transferred to the passive component. Near the stellar photosphere, the wind is relatively dense. From inspection of the frictional force (Eq. (6)), it follows that the drift velocity between absorbing ions and passive plasma can be low compared to the thermal speed of hydrogen. Consequently, frictional heating can be neglected in this region and the temperature structure is set mainly by the radiative processes and adiabatic cooling (see Drew 1989 for more detailed

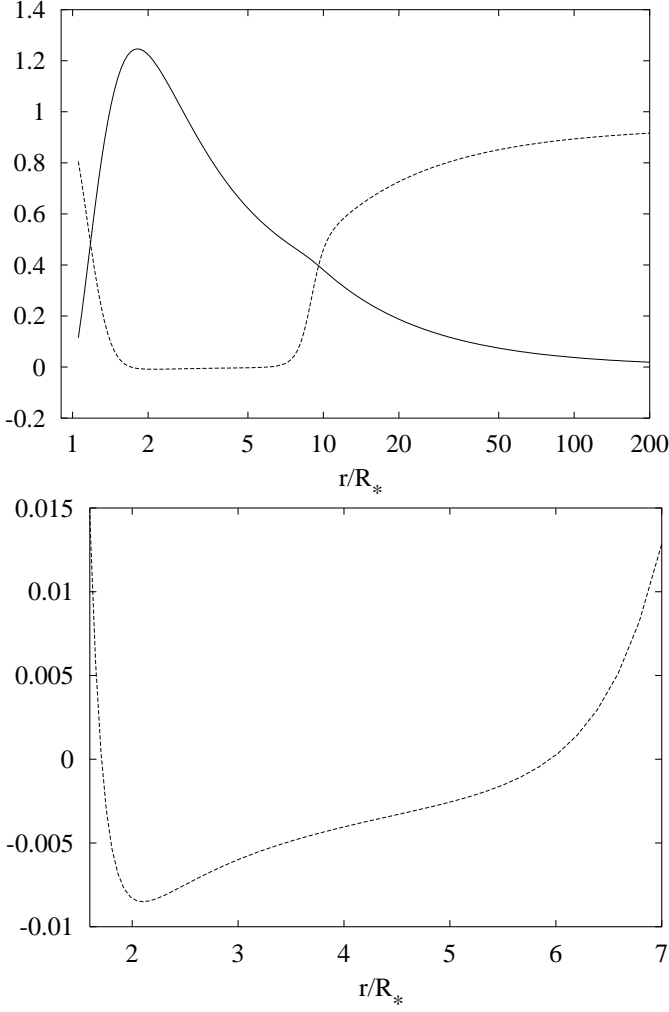


Fig. 4. Radiative heating or cooling (dashed line) and frictional heating (solid line) relative to the adiabatic cooling in the model of a B3 star wind. Note that in the range $2 R_* - 6 R_*$ the wind is slightly radiatively cooled (see the lower panel for detailed plot of radiative cooling in this region)

calculations). Hence, the three-component temperature is equal to its one-component value at the base of the wind.

However, this is not valid throughout the wind. At the outer parts of the wind the density decreases. Since the frictional force depends on the product of densities, the drift velocity should increase to accelerate the passive plasma (cf. Fig. 6 for the quantity x_{ip}). Consequently, frictional heating increases, but it also depends on the product of the densities of the interacting particles. Since the density of particles decreases, frictional heating reaches its maximum value and also decreases in the outermost parts of the wind. Therefore, at the outer parts of the wind the temperature is given by the balance between radiative heating and cooling and the three-component temperature is again equal to its one-component value. Finally, note that because $x_{ip} \approx 1$, the maximum of the Chandrasekhar function is not met anywhere in the wind. Thus, decoupling of radiatively accelerated ions and major passive component is excluded in such models.

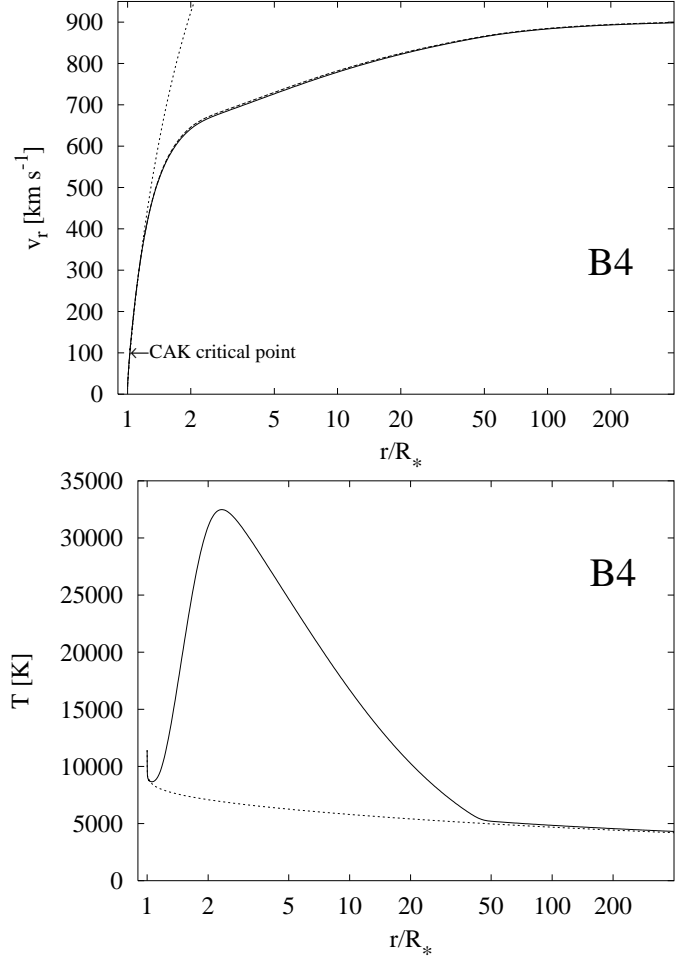


Fig. 5. The same as Fig. 1 for a B4 star. Heating is even greater than for a B3 star – cf. Fig. 3

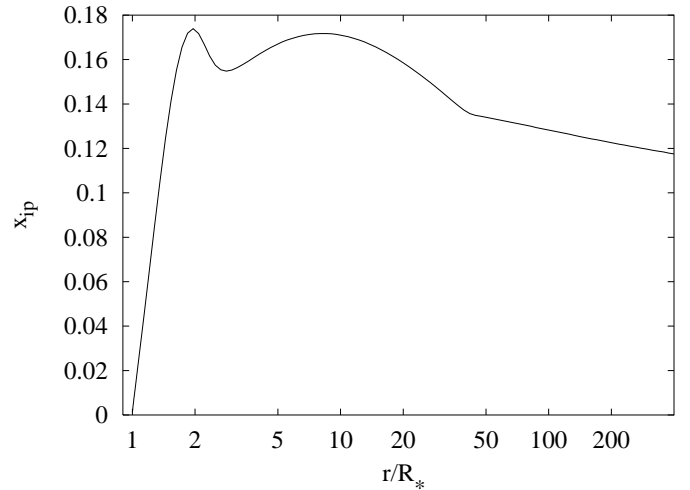


Fig. 6. The dependence of x_{ip} (see Eq. (10)) on radius for a B4 star

The behavior of individual heating or cooling terms is shown in Fig. 4. Note that in a particular case of a B3 star, radiative heating of a wind changes to radiative cooling in the domain of the wind where frictional heating is important. The most important component in frictional

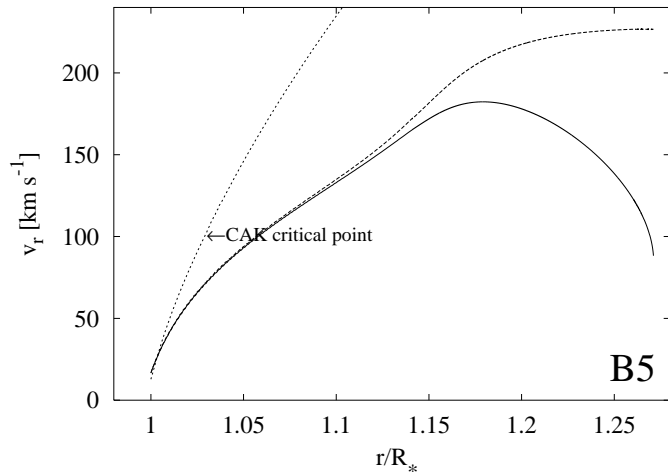


Fig. 7. The dependence of velocities on radius for a B5 star. The meaning of particular lines is same as in Fig. 1

heating is caused by encounters of non-absorbing and absorbing ions. Encounters of electrons and absorbing ions supply about two magnitudes less to frictional heating. Finally, frictional heating originating from encounters of non-absorbing ions and electrons is negligible due to the low drift velocity between these species.

Because the charge separation electric field is not a dominant term in momentum equations of both passive and active components, the electron component is only important in the temperature equation. Thus, the only effect of the electron component is a slight increase of temperature in the region where frictional heating is important. In most of our models, the electron velocity is very similar to the passive plasma velocity.

The velocity profile is affected by changes in the temperature structure through the dependence of radiative acceleration on the thermal speed (see Eq. (4)). The higher the temperature, the greater the thermal speed and the lower the radiative acceleration. Consequently, the wind terminal velocity decreases. Similarly Vink et al. (1999) concluded that lowering the radiative acceleration in the supersonic region leads to the lowering of the outflow velocity. To our knowledge, the effect of lowering of the outflow velocity by frictional heating is not mentioned anywhere in the literature.

3.3. Hydrogen backfalling to the stellar surface

At the lowest densities, the ionic component of the wind is unable to drag the passive plasma component out of the atmosphere, as displayed in Fig. 7. We see that the ionic and passive plasma decouple *well below* the point where the escape velocity is reached and the passive plasma falls back onto the stellar surface. However, this reaccretion should be studied using time-dependent calculations (cf. Porter & Skouza 1999). Moreover, for such low densities, a different type of solution is valid. As was shown by Babel (1996), the hydrostatic solution for passive plasma and the wind solution for absorbing ions exist simultaneously.

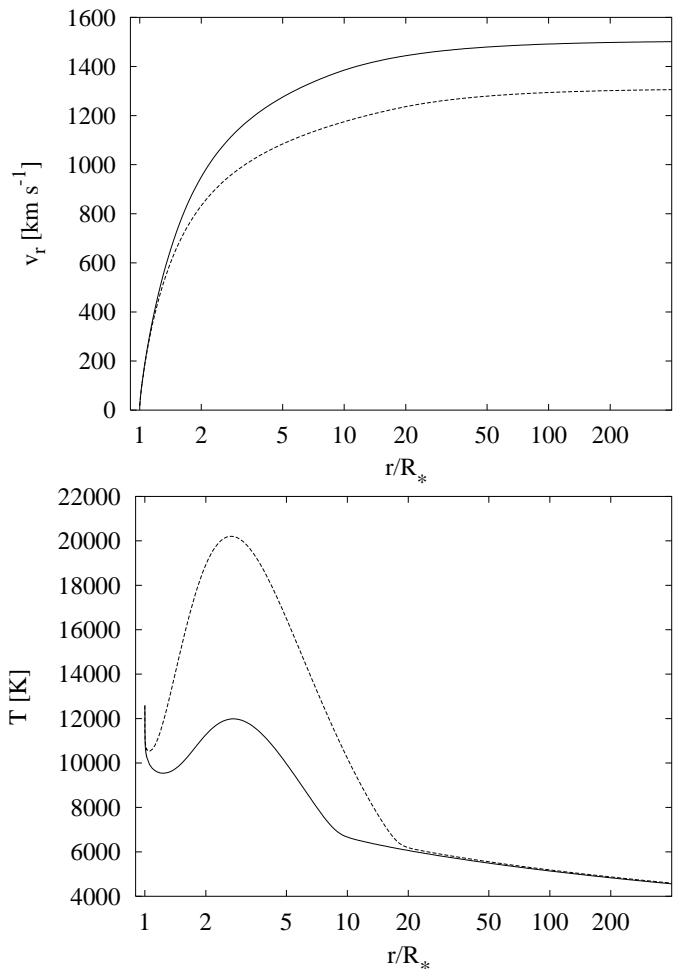


Fig. 8. Comparison of three-component models with (dashed line) and without (solid line) Doppler heating/cooling. Only ionic velocity is shown for both models

This type of solution was also studied for the case of a two-component wind (KK, model of B5 star with $q_i = 1.1 q_p$).

Only in this case does the resulting mass-loss rate of the three-component model differ significantly from its one-component value. Near the CAK point, temperature is higher almost by a factor of two than in the one-component case. As will be discussed in Sect. 4.3, a higher temperature below the CAK point lowers the mass-loss rate. In our particular case, the mass-loss rate computed in the three-component case is $4.9 \cdot 10^{-12} \mathcal{M} \text{ yr}^{-1}$, contrary to its one-component value $7.0 \cdot 10^{-12} \mathcal{M} \text{ yr}^{-1}$. Moreover, a lower temperature below the CAK point lowers the flow velocity and for this case the dependence of velocity on radius in one-component and three-component models differ significantly even *below* the critical point. This effect was enabled by including the variations in temperature and it is completely missing for isothermal winds in a two-component model (see KK and model of B5 star with $q_i = 1.1 q_p$ therein).

3.4. The effect of Doppler heating and cooling

However, there is another mechanism that is able to affect the thermal equilibrium of the wind, namely the Doppler heating (and cooling). This mechanism was studied in detail by Gayley & Owocki (1994). Doppler heating/cooling transfers energy directly from radiation to the motion of the atoms with the help of a difference between the absorption and emission frequency in a moving medium with a velocity gradient within the same line.

Inclusion of this effect requires a detailed knowledge of the line list (and, consequently, a huge amount of computer time), so we calculated only approximate values of the Doppler heating/cooling based on estimates from Gayley & Owocki (1994) in order to qualitatively estimate its effect. We added the Doppler heating/cooling term Q_{dh} into the radiative heating/cooling term Q^{rad} . For Q_{dh} we used the formula

$$Q_{\text{dh}} = \rho_i g_i^{\text{rad}} \sqrt{\frac{2kT}{m_i}} (w_{\text{dir}} - w_{\text{diff}}) \quad (42)$$

given by Gayley & Owocki (1994, Eq. (26) therein), where w_{dir} is a heating component of direct radiation and w_{diff} is a heating component of diffuse radiation. Note that their heating/cooling term \dot{q}_{dh} is defined per unit mass whereas Q_{dh} is defined per unit volume, so we inserted the term ρ_i . For the difference $w_{\text{dir}} - w_{\text{diff}}$ we used the rough estimate suggested by the same authors

$$w_{\text{dir}} - w_{\text{diff}} \approx 0.1. \quad (43)$$

We computed a B3 star model with inclusion of Doppler heating/cooling (see Fig. 8). The effect of Doppler heating/cooling is comparable to the effect of frictional heating and the total effect approximately doubles our temperature maximum. However, the qualitative picture of our results does not change. Detailed inclusion of Doppler heating/cooling as well as improved treatment of the line list will be dealt within our next paper(s).

4. General consequences of a multifluid approach

4.1. Dependence of force multipliers on metallicity

From the dependence of the radiative force in the multi-component approach (Eq. (4)) on the metallic density we can directly derive the dependence of the force-multipliers k , α on the metallicity. If the metallicity changes, then the actual metallic density is modified as

$$\rho_i = z \rho_{i\odot}, \quad (44)$$

where $\rho_{i\odot}$ is the corresponding solar value of the ion density and z is the actual abundance relative to its solar value. Consequently, the radiative acceleration acting on absorbing ions varies according to (see Eq. (4))

$$g_i^{\text{rad}} = z^{-\alpha} g_{i\odot}^{\text{rad}}. \quad (45)$$

Since the radiative force acting on the fluid in the one-component approximation is given by $\rho_i g_i^{\text{rad}}$, metallicity

effect can be described by the dependence of the force-multiplier k on the metallicity as

$$k = z^{1-\alpha} k_{\odot}, \quad (46)$$

which is the same result as obtained by Puls et al. (2000), who used the line statistics approach. This scaling law was also discussed by Abbott (1982).

4.2. Possible decoupling of individual components

Consider a situation in which the flow consists of two species, one of which is active and receives momentum (say, via radiative acceleration) and the second one is passive and is dragged via friction. Let us change the density in the wind (e.g. changing the boundary condition). For high densities, the frictional force is able to transfer sufficient amount of momentum from the active to the passive component. If the density is lower, then, because the velocity law is nearly the same, the frictional acceleration should be the same too. However, the corresponding density of the active component is now lower; therefore, to maintain the same frictional acceleration, the drift velocity between both components should be higher (see Eqs. (6), (7)). Apparently, this picture has its limitations. If the maximum of the Chandrasekhar function is reached, the frictional acceleration is not able to maintain the two-component flow. The behavior of the velocity law out of this point depends generally on the densities of both components and on the force acting on active component. This will be discussed for two basic different cases below.

4.2.1. The major active component

If the density of the active component is significantly higher than the density of the passive component, then decoupling of the passive component from the major flow is possible. This can be seen easily from the equation of motion of the active component (Eq. (2)). The friction term can be neglected because the passive plasma density is substantially lower than the active plasma density and therefore the passive component does not influence the active component. Contrary, lowering of the frictional term in the equation of motion of a passive component should be balanced by lowering of the passive plasma velocity gradient, i.e. decoupling is possible. Clearly, if the passive component reaches the escape velocity, then it leaves the star separately; if its velocity is lower than the actual escape velocity then the passive component falls back onto the star.

Interestingly, the point where the minor component decouples from the main flow does not depend on its density. This can be seen easily from the equation of motion (2) of the minor component. The only term which depends on the minor component density is the gas pressure term, which can be neglected. Thus, if the wind is not significantly heated during decoupling, the point where the minor component decouples does not depend on its density.

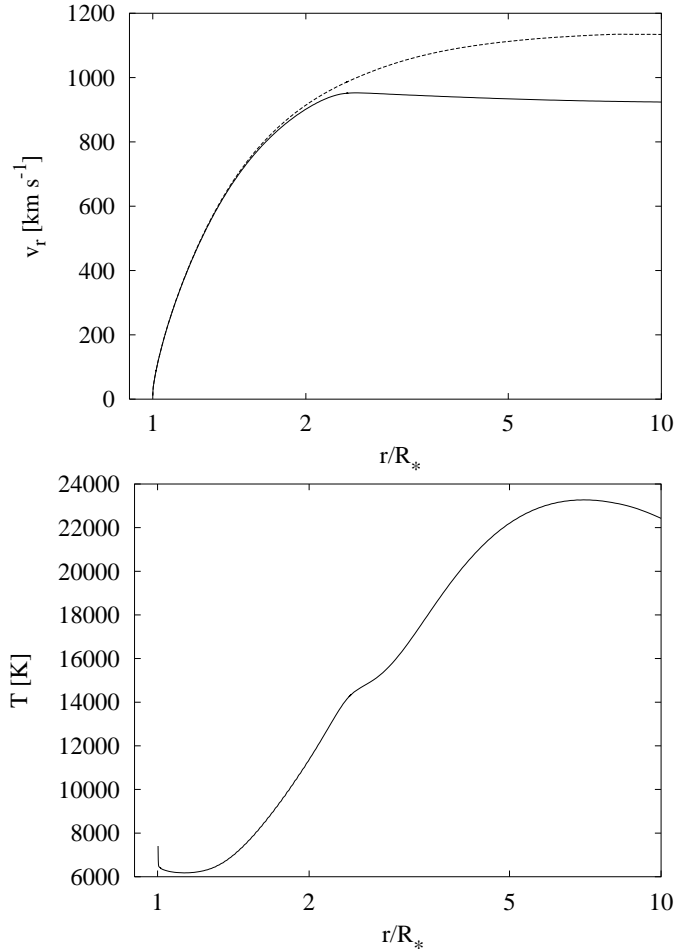


Fig. 9. Wind model with major active component (dashed line) allowing for decoupling of the passive component (solid line)

The location of this point depends on the mass and charge of both components and on the major component density. However, in this case, we completely neglected the effect of frictional heating. Therefore, the situation described may be generally more complicated, especially if the force acting on the major component depends on temperature (as the line-force actually does).

To manifest such theoretical results we computed a wind model of a B3 star (using parameters listed in the Table 1) with an artificially enhanced ion-to-hydrogen ratio of $\mathfrak{Q}_i = 100$. The numerical model obtained in Fig. 9 supports preceding theoretical considerations. Both components decouple. Moreover, the wind is significantly heated, attaining a maximum temperature of about 23 000 K.

4.2.2. The minor active component

The situation is completely different in the case when the component receiving the major amount of momentum is a minor element relative to the passive plasma. This is the common case in the radiatively driven stellar wind. At the point where the Chandrasekhar function reaches its maximum, frictional acceleration is not capable of transferring

sufficient amount of momentum to the passive plasma. Quantitatively, the frictional force is lower by ΔR compared to the case when it is capable of maintaining the common flow of both components. Therefore, the velocity gradient of the passive component p should drop by $\Delta(dv_{rp}/dr)$. The equation of motion yields

$$\left(v_{rp} - \frac{a_p^2}{v_{rp}}\right) \Delta \frac{dv_{rp}}{dr} = \frac{\Delta R}{\rho_p},$$

where the continuity equation was used. This decrease of the frictional force also affects the active component. For the change in the velocity gradient of active plasma $\Delta dv_{ri}/dr$ we can write (from the equation of motion of the active plasma)

$$\left(v_{ri} - \frac{a_i^2}{v_{ri}}\right) \Delta \frac{dv_{ri}}{dr} = \Delta g_R - \frac{\Delta R}{\rho_i},$$

where Δg_R is the change of force that drives active plasma. Such a picture is valid for both isothermal and nonisothermal wind. However, especially in the latter case, it should be justified by numerical calculations. Generally, there are two possible cases of downstream flow, based on whether the driving force depends on the velocity gradient or not.

Constant driving force. First, we assume that the driving force g_R does not depend on the velocity gradient dv_{ri}/dr . Then the velocity gradient should change substantially, given that in this region $v_{ri} \approx v_{rp}$ and the change of the active component velocity gradient reads

$$\Delta \frac{dv_{ri}}{dr} = -\frac{\rho_i}{\rho_p} \frac{dv_{ri}}{dr}.$$

In this case, decoupling is possible. To prove this conclusion, we computed nonisothermal models with constant acceleration (i.e. acceleration which does not depend on the velocity gradient). We selected a model of a B3 star and as the driving acceleration we chose the radiative force in the CAK approximation computed for the beta-velocity law with $\beta = 0.45$ and $v_\infty = 1100 \text{ km s}^{-1}$. This computed force we held fixed during Newton-Raphson iterative steps. For high values of q_i for which the Chandrasekhar function does not reach its maximum, no decoupling occurs. On the other hand, for low values of ionic charge q_i for which friction is not capable of driving the passive plasma flow, runaway of ions occurs, enabled by steep increase in the ionic velocity gradient, as was already discussed (see Fig. 10). Finally, the friction heats the flow, increasing the wind temperature by orders of magnitude. This offers a plausible model of how wind temperatures sufficient to produce X-rays can be attained.

Driving force increasing with the velocity gradient. On the other hand, if the driving force is an increasing function of the velocity gradient, then an abrupt increase of the velocity gradient of the active component (contrary to the previous case) enhances the driving force and further disrupts the momentum balance. Therefore, in this case, the

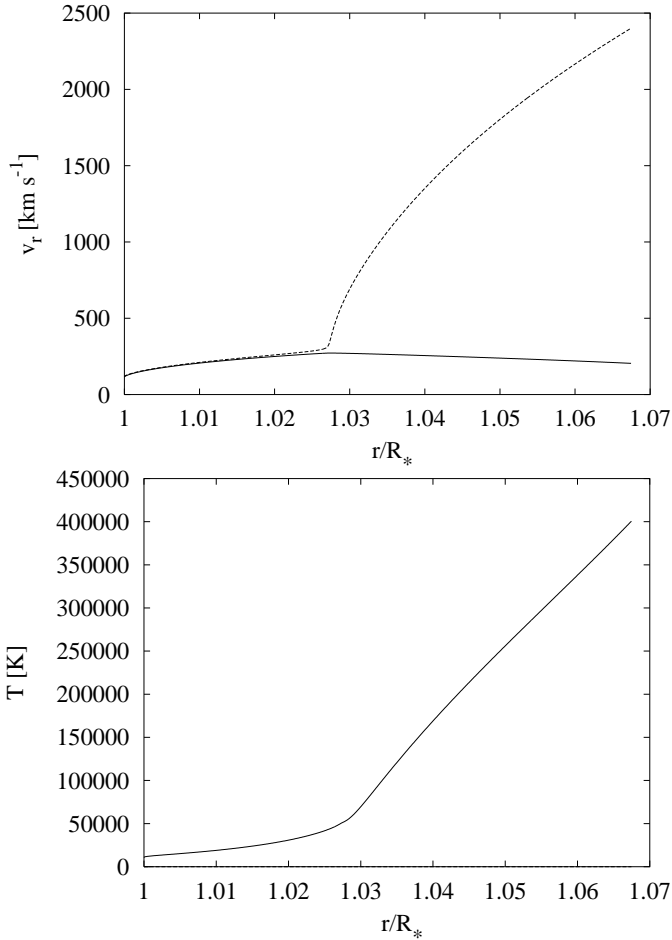


Fig. 10. Model of a B3 star wind with constant driving acceleration for $q_i = 0.6q_p$ (see the text). The notation is the same as in Fig. 1

momentum balance would not be achieved by an increase of the velocity gradient, but rather by a decrease. The velocity gradient should drop according to

$$\left(v_{ri} - \frac{a_i^2}{v_{ri}} - \frac{\partial g_R}{\partial (dv_{ri}/dr)} \right) \Delta \frac{dv_{ri}}{dr} = - \frac{\Delta R}{\rho_i}.$$

If the first two left-hand side terms can be neglected (as in the case of the radiative force in the Sobolev approximation, see KK), the above equation can be rewritten

$$\Delta g_R \equiv \frac{\partial g_R}{\partial (dv_{ri}/dr)} \Delta \frac{dv_{ri}}{dr} = \frac{\Delta R}{\rho_i}.$$

In the case of the Sobolev approximation this means that the active component velocity gradient drops and decoupling is not possible. Thus, in the supersonic flow, the possibility of ion runaway crucially depends on the driving force.

However, this conclusion cannot be proved in the non-isothermal case, due to the dependence of radiative acceleration on temperature. When the velocity difference between active and passive components rises, the wind is significantly heated by friction and the radiative acceleration is lower. This decreases the outflow velocity and

increases wind density such that the Chandrasekhar function *does not reach its maximum value* and thus even the possibility of decoupling is excluded (see Sect. 3.2).

4.2.3. Nearly equal densities of both components

The most complicated situation occurs when the densities of both active and passive components are nearly equal. In this case, the above-mentioned equations cannot be used in such a simple form because the possibility of decoupling crucially depends on the functional dependence of the driving force, i.e. dependence on the velocity gradient, temperature etc. The question of whether decoupling is possible or not should thus be solved only using careful numerical computations. However, the latter case probably has limited astrophysical relevance, because hydrogen is the most abundant element in the majority of stars. On the other hand, there exists an interesting class of hydrogen-deficient stars where the case of nearly equal densities may occur. However, such analysis, although interesting, goes far beyond the scope of this paper.

4.3. Mass-loss rate

Since condition (28), used to fix the mass-loss rate in the case when both components are coupled (i.e. $v_{rp} \approx v_{ri}$ and $dv_{rp}/dr \approx dv_{ri}/dr$) is nearly the same as the CAK condition (41), the three-component mass loss rate and the one-component mass loss rate (showed in the Table 2) in this limit are nearly the same. Moreover, a condition (28) leads to a maximum mass-loss rate, for which a stable solution exists, similar to the one-component case (see Poe et al. 1990).

Table 2. Mass-loss rates of one-component (1C) and three-component (3C) models. All values are $\mathfrak{M}_{\odot} \text{ yr}^{-1}$

Star	B0	B1	B2	B3	B4	B5	τ Sco
1C	$3 \cdot 10^{-8}$	$1 \cdot 10^{-8}$	$4 \cdot 10^{-9}$	$4 \cdot 10^{-10}$	$6 \cdot 10^{-11}$	$7 \cdot 10^{-12}$	$1 \cdot 10^{-8}$
3C	$3 \cdot 10^{-8}$	$1 \cdot 10^{-8}$	$4 \cdot 10^{-9}$	$4 \cdot 10^{-10}$	$6 \cdot 10^{-11}$	$5 \cdot 10^{-12}$	$1 \cdot 10^{-8}$

This is not true in the case when the gas is significantly heated by friction near the CAK point. Higher temperature increases thermal speed and therefore decreases radiative acceleration in the Sobolev approximation Eq. (4). As was discussed by Vink et al. (1999), as the line acceleration in the subsonic region decreases, mass-loss rate decreases.

It is interesting to discuss the influence of heating on the observed mass-loss rates. Recent detailed theoretical study of mass-loss rates of Vink et al. (2000) showed that there is a quite good agreement between theoretical mass-loss rates for O stars and mass-loss rates deduced from radio emission and H α profile. On the other hand, theoretical mass-loss rates for B stars are in good agreement with mass-loss rates calculated from radio emission

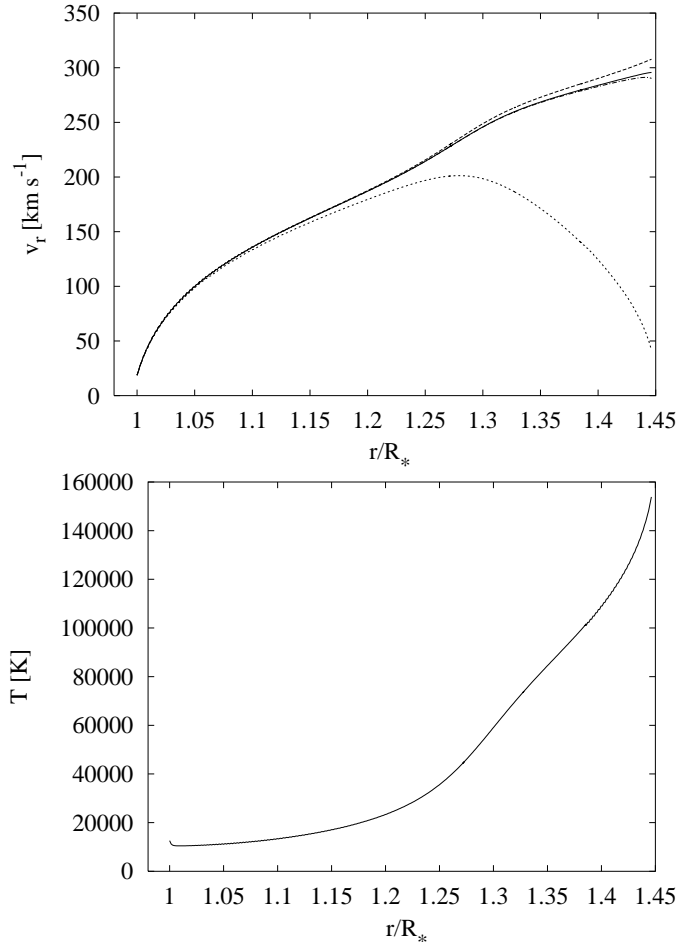


Fig. 11. Decoupling of helium (dotted line) from common hydrogen (solid line) and absorbing ion (dashed line) flow in the model of a B3 star four-component wind. In the outermost parts of the wind the electron velocity (dashed-dotted line) differs slightly from the hydrogen velocity

(Scuderi et al. 1998) but not with mass-loss rates deduced from $H\alpha$ profiles (Kudritzki et al. 1999). Since the radio emission originates at several hundred stellar radii (Lamers & Leitherer 1993) where the radiative equilibrium holds (see Fig. 5), the “radio mass-loss rates” are not affected by frictional heating. However, the $H\alpha$ line originates from layers closer to the star and therefore can be affected by frictional heating. Thus, proper inclusion of the frictional (and possibly Doppler) heating can help understanding of the discrepancy between mass-loss determined by various methods for B stars.

5. Applications of three-component model

5.1. Decoupling of helium

The interesting paper of Hunger & Groote (1999) motivated us to test whether we are also able to predict decoupling of helium on the basis of our multicomponent model. Therefore we introduced two new variables to describe the helium flow, namely helium density ρ_{He} and helium radial velocity $v_{r,\text{He}}$. We assumed helium atoms

to have mass $m_{\text{He}} = 4m_{\text{p}}$ and charge q_{He} . The helium velocity and density are obtained from continuity Eq. (1) and equation of motion Eq. (2). We added appropriate helium terms into the energy Eq. (15) and into the critical point condition Eq. (28). We assumed a solar abundance of helium at the base of the wind and equal base velocities of helium and hydrogen. The ion velocity is determined as described in Sect. 2.5.2. We stress that these models are not fully self-consistent because we did not include the helium critical point. This is completely beyond the scope of the present article; we aim only to show that helium decoupling from the main absorbing ions – hydrogen flow is possible. Detailed calculations of a four-component model including helium will be published elsewhere.

The model of the four-component flow in a B3 star is given in Fig. 11 for $q_{\text{He}} = 0.03q_{\text{p}}$. At a point where the common flow of hydrogen and absorbing ions is not able to support helium flow, the latter decouples from the other components and its velocity decreases. Because the helium velocity is *lower* than the escape velocity, helium can reaccrete to the star, creating possible surface helium overabundance if magnetic fields are present (Hunger & Groote 1999) or possible He shells (Porter & Skouza 1999). Note that such stationary models cannot be extended to an arbitrary radius. During deceleration the helium critical point is again reached, and further operation of the gravitational force reverses the direction of the helium flow and causes its backfalling to the stellar surface. Such a situation cannot be correctly described by our model.

The wind is significantly heated by friction between helium and other components beyond the point where helium decouples from the main flow. Higher temperatures would lower the argument x_{pi} of the Chandrasekhar function (see Eq. (10)) and therefore lower the frictional force between hydrogen and metallic components. Thus, to maintain a common flow of hydrogen and absorbing ions, the drift velocity should increase.

Helium decoupling is sensitive to the helium charge and therefore to the temperature. For such low temperatures, which are commonly attained in the stellar wind of B stars, decoupling would be possible. However, if the helium charge would rise (due to higher wind temperature) e.g. to $q_{\text{He}} = q_{\text{p}}$ no helium decoupling would occur. Thus, the detailed picture of helium decoupling is much more complicated and needs further study.

If the present picture of helium decoupling is correct, then Bp and Ap stars with winds could be X-ray sources. Recently this was justified by Dachs & Hummel (1996) for the case of the young open cluster NGC 2516. Unfortunately, it is not clear if the source of the X-rays are Bp stars themselves or their possible cool companions with hot coronae.

5.2. τ Sco

This well-studied star is a puzzling object. Although it became a benchmark star for theoretical and observational

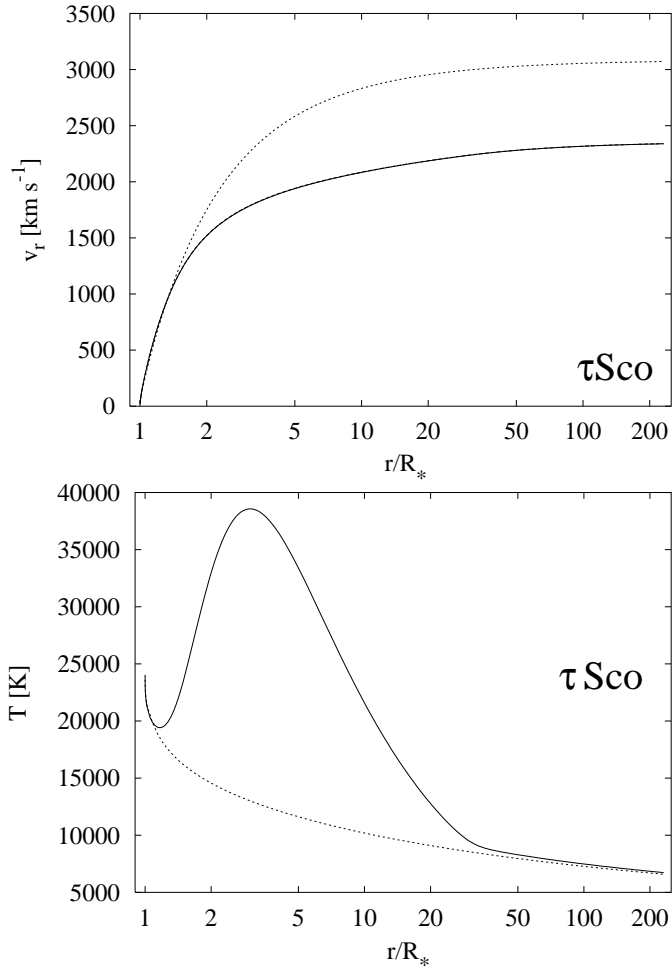


Fig. 12. Three-component wind model of τ Sco. The notation is the same as in Fig. 1. Note that inclusion of frictional heating lowers the outflow velocity towards observed values

studies, its nature is not yet well known. The observed terminal velocity estimate – about 2000 km s^{-1} (Abbott 1978; Lamers & Rogerson 1978) contradicts the value 3850 km s^{-1} obtained from a detailed theoretical study by Pauldrach (1987). Springmann & Pauldrach (1992) were able to reduce the theoretical value using the two-component model of the stellar wind, however, using a lower value of a mass-loss rate.

Our one-component model with much simpler atomic physics than Pauldrach (1987) predicts a terminal velocity 3000 km s^{-1} , well above the experimental result. Therefore, we computed a three-component model of this star to find out if our models are able to explain the low terminal velocity of this star. According to Kilian (1994), we reduced the metallicity to the value $z = 0.6$. Unfortunately, even such a three-component model yielded nearly the same value for terminal velocity as the one-component model. Therefore, we assumed slightly reduced metallicity contrary to Kilian, $z = 0.3$, to allow for greater frictional heating. This artificial change of the metallicity does not indicate our mistrust of observed metallicity values. Rather it indicates that our model

assumptions (e.g. the representative nature of our ions) do not correspond to the reality of τ Sco. We believe more detailed models in the future can explain the low terminal velocity of τ Sco more precisely. Nevertheless, based on these assumptions, we showed that frictional heating may play an important role in the model of τ Sco wind because it reduces its terminal velocity to 2400 km s^{-1} , closer to the observed values. Moreover, the computed velocity profile (see Fig. 12) is very similar to that derived from a detailed UV-line fit by Hamann (1981).

We would like to emphasize that our computed low value for the terminal velocity was not obtained due to the reduced value of metallicity, because our wind model with $z = 0.3$ without frictional heating yields nearly the same terminal velocity as the one-component model with $z = 1.0$. The low value of terminal velocity was obtained due to the inclusion of frictional heating into our models. Although Springmann & Pauldrach (1992) also explained the low terminal velocity of τ Sco on the basis of multicomponent flow, our approach is substantially different, their explanation being on ion runaway. Another problem arising for other low-density wind stars is the determination of the mass-loss rate. Our obtained value, $1.2 \cdot 10^{-8} \mathcal{M}_\odot \text{ yr}^{-1}$, is about a factor of 3 lower than that obtained from the usual CAK approximation (see e.g. Cohen et al. 1997, who used the “cooking formula” of Kudritzki et al. 1989), due to the reduced metallicity in our models. This value is slightly higher than a new upper-limit of the mass-loss rate, $6 \cdot 10^{-9} \mathcal{M}_\odot \text{ yr}^{-1}$, constrained by Zaal et al. (1999) from infrared emission; however, this result is sensitive to a star’s effective temperature.

Finally, Waters et al. (1993) reported the presence of hydrogen emission lines in the infrared spectrum of τ Sco and concluded that τ Sco is a pole-on Be star. However, Murdoch et al. (1994) suggested that infrared hydrogen emission is caused by the presence of NLTE effects (see also Zaal et al. 1999). Our NLTE spherically-symmetric static model of the photosphere of τ Sco predicts infrared emission both in hydrogen and helium lines.

6. Conclusions

We computed three-component models of a radiatively driven wind of hot B stars. We showed that friction has a negligible effect in high density winds, i.e. in stars with a relatively high mass-loss rate. For these stars, three-component calculations yield the same results as the common one-component ones.

For low density winds the inclusion of friction leads to heating of the flow. We showed that in self-consistent hydrodynamic models, friction can heat the gas to temperatures up to two times the effective temperature. This heating leads to lowering of the radiative force and, consequently, to the lowering of the outflow velocity. Lower outflow velocity leads to higher density and this means, together with higher thermal speed, that the drift velocity of both components is too low to allow decoupling of passive and absorbing components.

Finally, stars where absorbing plasma is not able to drag the passive plasma out from the atmosphere have a purely metallic wind, as has already been shown by Babel (1995, 1996).

We derived general conditions for decoupling of a multicomponent flow. We showed that if the density of the accelerated component is higher than the density of the passive component, then decoupling is possible, regardless of the actual form of driving force. On the other hand, if the density of the accelerated component is lower than the density of the passive component, then the possibility of decoupling is given by the functional dependence of the driving force. If the driving force does not change substantially in the region where decoupling is possible, then decoupling of individual components is again possible. If the driving force scales with velocity gradient (as in the Sobolev approximation), then decoupling of individual components is not possible.

Our calculations indicate that friction is able to heat the wind to the temperatures of the order of 10^6 K (see Fig. 10). Such a hot medium is able to emit X-ray radiation. However, quantitative estimates of X-ray luminosity are beyond the scope of this paper.

There are many applications of the multifluid model of stellar wind. Considering helium as a fourth component, one can apply the model of a multicomponent wind to the study of chemically peculiar stars. We are also able to fit the outflow velocity of the star τ Sco closer to the observed value.

Unfortunately, our approach of handling the problem is still not satisfactory. Mainly, the approximation of one-type absorbing ions with parameters which are not rigidly given may lead to some misunderstanding. The approximation of constant ionic charge is not self-consistent because the degree of ionization changes with temperature and density. Moreover, allowing for a macroscopic electric field may lead to some observable effects (Porter 1999, private communication). Such studies with the inclusion of inspection of stability of multicomponent flow will be the subject of future papers. However, we are now able to describe the general picture of multifluid flow, which will likely not be strongly affected by future refinements.

Acknowledgements. The authors would like to thank Dr. John Porter for his comments on the manuscript. This research made use of NASA's Astrophysics Data System Abstract Service (Kurtz et al. 2000; Eichhorn et al. 2000; Accomazzi et al. 2000; Grant et al. 2000). This work was supported by projects K1-003-601/4 and K1-043-601.

Appendix A: Details of numerical method

The non-linear operator \mathbf{P} has following form:

– for $i = 1$

$$P_1 = \rho_{i1} - \rho_0 \quad (\text{A.1a})$$

$$P_2 = \frac{G\mathfrak{M}}{r_1^2} (1 - \Gamma) - \frac{4a_p^2}{r_1} + \mathcal{R}_{pi} \ln \Lambda + \frac{m_e}{m_p} \mathcal{R}_{ei} \ln \Lambda \quad (\text{A.1b})$$

$$P_3 = \rho_{p1} - \frac{1}{\mathfrak{Y}_i} \rho_{i1} \frac{v_{ri1}}{v_{rp1}}, \quad (\text{A.1c})$$

$$P_4 = v_{rp1}(R_*) - sa_p, \quad (\text{A.1d})$$

$$P_5 = \rho_{e1} - \frac{m_e}{m_p} \left(\rho_{p1} + \frac{z_i}{A_i} \rho_{i1} \right), \quad (\text{A.1e})$$

$$P_6 = \rho_{e1} v_{re1} - \frac{m_e}{m_p} \left(\rho_{p1} v_{rp1} + \frac{z_i}{A_i} \rho_{i1} v_{ri1} \right) \quad (\text{A.1f})$$

$$P_7 = Q^{\text{rad}}. \quad (\text{A.1g})$$

– for $1 < i < \text{NR}$

$$P_{7i-6} = \left[\frac{d(r^2 \rho_i v_{ri})}{dr} \right]_i \quad (\text{A.2a})$$

$$P_{7i-5} = v_{ri,i} \left[\frac{dv_{ri}}{dr} \right]_i + \frac{a_i^2}{\rho_{i,i}} \left[\frac{d\rho_i}{dr} \right]_i + \left[\frac{da_i^2}{dr} \right]_i - \frac{q_i}{m_i} E - x_{i\alpha} \left(\frac{1}{\rho_{i,i}} \left[\frac{dv_{ri}}{dr} \right]_i \right)^\alpha + g + (\mathcal{R}_{ip} + \mathcal{R}_{ie}) \ln \Lambda \quad (\text{A.2b})$$

$$P_{7i-4} = \left[\frac{d(r^2 \rho_p v_{rp})}{dr} \right]_i \quad (\text{A.2c})$$

$$P_{7i-3} = v_{rp,i} \left[\frac{dv_{rp}}{dr} \right]_i + \frac{a_p^2}{\rho_{p,i}} \left[\frac{d\rho_p}{dr} \right]_i + \left[\frac{da_p^2}{dr} \right]_i - \frac{q_p}{m_p} E + g + \mathcal{R}_{pi} \ln \Lambda + \mathcal{R}_{pe} \ln \Lambda \quad (\text{A.2d})$$

$$P_{7i-2} = \rho_{e,i} - \frac{m_e}{m_p} \left(\rho_{p,i} + \frac{z_i}{A_i} \rho_{i,i} \right), \quad (\text{A.2e})$$

$$P_{7i-1} = \rho_{e,i} v_{re} - \frac{m_e}{m_p} \left(\rho_{p,i} v_{rp,i} + \frac{z_i}{A_i} \rho_{i,i} v_{ri,i} \right), \quad (\text{A.2f})$$

$$P_{7i} = \frac{3}{2} k \left[\frac{dT}{dr} \right]_i \sum_{a=p,e,i} v_{ra,i} \frac{\rho_{a,i}}{m_a} + \sum_{a=p,e,i} a_a^2 \rho_{a,i} \frac{1}{r_i^2} \left[\frac{d(r^2 v_{ra})}{dr} \right]_i - Q^{\text{rad}} - \frac{1}{2} \sum_{a=p,e,i} \sum_{\substack{b=p,e,i \\ b \neq a}} \rho_a \mathcal{R}_{ab} \ln \Lambda (v_{ra,i} - v_{rb,i}). \quad (\text{A.2g})$$

– for $i = \text{NR}$

$$P_{7i-6} = \left[\frac{d(r^2 \rho_i v_{ri})}{dr} \right]_i \quad (\text{A.3a})$$

$$P_{7i-5} = \frac{v_{ri,i} - v_{ri,i-1}}{\Delta r_i} - \frac{v_{ri,i-1} - v_{ri,i-2}}{\Delta r_{i-1}} \quad (\text{A.3b})$$

$$P_{7i-4} = \left[\frac{d(r^2 \rho_p v_{rp})}{dr} \right]_i \quad (\text{A.3c})$$

$$P_{7i-3} = \frac{v_{rp,i} - v_{rp,i-1}}{\Delta r_i} - \frac{v_{rp,i-1} - v_{rp,i-2}}{\Delta r_{i-1}} \quad (\text{A.3d})$$

$$P_{7i-2} = \rho_{e,i} - \frac{m_e}{m_p} \left(\rho_{p,i} + \frac{z_i}{A_i} \rho_{i,i} \right), \quad (\text{A.3e})$$

$$P_{7i-1} = \rho_{e,i} v_{re} - \frac{m_e}{m_p} \left(\rho_{p,i} v_{rp,i} + \frac{z_i}{A_i} \rho_{i,i} v_{ri,i} \right), \quad (\text{A.3f})$$

$$P_{7i} = \frac{T_i - T_{i-1}}{\Delta r_i} - \frac{T_{i-1} - T_{i-2}}{\Delta r_{i-1}}. \quad (\text{A.3g})$$

We used following abbreviations:

$$\left[\frac{dX}{dr} \right]_i = \begin{cases} y_i \frac{X_{i+1} - X_i}{\Delta r_{i+1}} + (1 - y_i) \frac{X_i - X_{i-1}}{\Delta r_i}, & i < \text{NR}, \\ \frac{X_i - X_{i-1}}{\Delta r_i}, & i = \text{NR}, \end{cases} \quad (\text{A.4a})$$

where X stands for v_{ri} , v_{rp} , ρ_i , ρ_p etc.

$$\Delta r_i = r_i - r_{i-1}, \quad (\text{A.4b})$$

$$y_i = \frac{r_i - \bar{r}_i}{\bar{r}_{i+1} - \bar{r}_i}, \quad (\text{A.4c})$$

$$\bar{r}_i = \frac{1}{2} (r_i + r_{i-1}) \quad (\text{A.4d})$$

$$x_{i\alpha} = \frac{1}{\mathfrak{Y}_i} \frac{\sigma_e L}{4\pi r^2 c} \left(\frac{1}{10^{11} \text{ cm}^{-3}} \frac{\rho_e}{m_e W} \right)^\delta \times \frac{(1 + \sigma_i)^{\alpha+1} - (1 + \sigma_i \mu_c^2)^{\alpha+1}}{(\alpha + 1)(1 - \mu_c^2) \sigma_i (1 + \sigma_i)^\alpha} k \left(\frac{\mathfrak{Y}_i}{\sigma_e v_{\text{th}}} \right)^\alpha \quad (\text{A.4e})$$

$$\sigma_i = \frac{r_i}{v_{ri}} \left[\frac{dv_{ri}}{dr} \right]_i - 1 \quad (\text{A.4f})$$

$$\mathcal{R}_{ab} = \rho_b \frac{4\pi q_a^2 q_b^2}{m_a m_b k T} \frac{v_{ra} - v_{rb}}{|v_{ra} - v_{rb}|} G(x_{ab}) \quad (\text{A.4g})$$

where a, b , stands for i, p, e

$$\ln \Lambda = \ln \left(24\pi \sqrt{\frac{m_p}{\rho_i}} \left(\frac{kT}{4\pi e^2} \right)^{3/2} \right) \quad (\text{A.4h})$$

$$\tilde{\rho}_i = \rho_{p,i} + \frac{m_p}{m_e} \rho_{e,i} + \frac{m_p}{m_i} \rho_{i,i} \quad (\text{A.4i})$$

$$E = \frac{m_e}{e} \left(g_e^{\text{rad}} - g - \left[\frac{da_e^2}{dr} \right]_i - \frac{a_e^2}{\rho_e} \left[\frac{d\rho_e}{dr} \right]_i - \mathcal{R}_{ep} \ln \lambda - \mathcal{R}_{ei} \ln \lambda \right) \quad (\text{A.4j})$$

$$Q^{\text{rad}} = 4\pi n_{e,i} n_{p,i} \sum_{j=1}^{NFR} \alpha_{\text{ff}}(\nu_j, T_i) \times \left[J_j - \left(J_j + \frac{2h\nu_j^3}{c^2} \right) e^{-h\nu_j/kT_i} \right] \Delta\nu_j + 4\pi \sum_{l=1}^2 n_{l,i} \sum_{j=1}^{NFR} \alpha_{\text{bf},l}(\nu_j) \times \left[J_j - \left(J_j + \frac{2h\nu_j^3}{c^2} \right) e^{-h\nu_j/kT_i} \right] \times \left[1 - \frac{\nu_l}{\nu_j} \right] \Delta\nu_j \quad (\text{A.4k})$$

$$s^2 = 1 + \frac{n_p}{n_e} \left[z_p^2 + \frac{2}{3} (1 + z_p) \frac{n_e (v_{rp} + z_p v_{re})}{\sum_{b \neq e} (1 + z_b) n_b v_{rb}} \right] \quad (\text{A.4l})$$

where i denotes i th point of the grid. In some circumstances (when the argument of the Chandrasekhar function is comparable with the thermal speed) it is convenient to introduce the new independent variable $\Delta v_r = v_{ri} - v_{rp}$

and use this variable in the linearization and computation of the Chandrasekhar function.

For a calculation of the model below the critical point we typically use $\text{NR} = 50$ grid points, whereas for the model above the critical point we use $100 \leq \text{NR} \leq 200$ grid points. In both cases, the grid points are spaced logarithmically (although this leads to nearly linear placement of grid points in the former case).

References

- Abbott, D. C. 1978, *ApJ*, 225, 893
 Abbott, D. C. 1980, *ApJ*, 242, 1183
 Abbott, D. C. 1982, *ApJ*, 259, 282
 Accomazzi, A., Eichhorn, G., Kurtz, M. J., Grant, C. S., & Murray, S. S. 2000, *A&AS*, 143, 85
 Babel, J. 1995, *A&A*, 301, 823
 Babel, J. 1996, *A&A*, 309, 867
 Beutler, G. 1979, *Numerische Integration von gewöhnlichen Differentialgleichungen*, Mitt. Satell.-Beobachtungsstn. Zimmerwald, 4, Astron. Inst., Univ. of Bern, Bern, Switzerland
 Braginskij, S. I. 1963, in *Voprosy teorii plazmy*, vol. 1, ed. M. A. Leontovich, Gosatomizdat, Moskva, 183
 Bürgi, A. 1992, *J. Geophys. Res.*, 97, 3137
 Castor, J. I., Abbott, D. C., & Klein, R. I. 1975, *ApJ*, 195, 157 (CAK)
 Cohen, D. H., Cassinelli, J. P., & Waldron, W. L. 1997, *ApJ*, 488, 397
 Dachs, J., & Hummel, W. 1996, *A&A*, 312, 818
 Dreicer, H. 1959, *Phys. Rev.*, 115, 238
 Drew, J. E. 1985, *MNRAS*, 217, 867
 Drew, J. E. 1989, *ApJS*, 71, 267
 Eichhorn, G., Kurtz, M. J., Accomazzi, A., Grant, C. S., & Murray, S. S. 2000, *A&AS*, 143, 61
 Friend, D. B., & Abbott, D. C. 1986, *ApJ*, 311, 701
 Grant, C. S., Accomazzi, A., Eichhorn, G., Kurtz, M. J., & Murray, S. S. 2000, *A&AS*, 143, 111
 Gayley, K. G., & Owocki, S. P. 1994, *ApJ*, 434, 684
 Hamann, W.-R. 1981, *A&A*, 100, 169
 Harmanec, P. 1988, *Bull. Astron. Inst. Czechosl.*, 39, 329
 Henyey, L. G., Forbes, J. E., & Gould, N. L. 1964, *ApJ*, 139, 306
 Hunger, K., & Groote, D. 1999, *A&A*, 351, 554
 Kilian, J. 1994, *A&A*, 282, 867
 Krtička, J., & Kubát, J. 2000, *A&A*, 359, 983 (KK)
 Kubát, J. 2001, *A&A*, 366, 210
 Kubát, J., Puls, J., & Pauldrach, A. W. A. 1999, *A&A*, 341, 587
 Kudritzki, R. P., Pauldrach, A. W. A., Puls, J., & Abbott, D. C. 1989, *A&A*, 219, 205
 Kudritzki, R. P., Puls, J., Lennon, D. J., et al. 1999, *A&A*, 350, 970
 Kurtz, M. J., Eichhorn, G., Accomazzi, A., et al. 2000, *A&AS*, 143, 41
 Lamers, H. J. G. L. M., & Leitherer, C. 1993, *ApJ*, 412, 771
 Lamers, H. J. G. L. M., & Rogerson, J. B. 1978, *A&A*, 66, 417
 Lang, K. R. 1974, *Astrophysical Formulae* (Springer-Verlag, Berlin)
 Lucy, L. B., & Solomon, P. M. 1970, *ApJ*, 159, 879
 Mihalas, D. 1978, *Stellar Atmospheres*. 2nd ed. (W. H. Freeman Comp., San Francisco)

- Murdoch, K. A., Drew, J. E., & Anderson, L. S. 1994, *A&A*, 284, L27
- Nobili, L., & Turola, R. 1988, *ApJ*, 333, 248
- Owocki, S. P., Cranmer, S. R., & Blondin, J. M. 1994, *ApJ*, 424, 887
- Pauldrach, A. W. A. 1987, *A&A*, 183, 295
- Pauldrach, A., Puls, J., & Kudritzki, R. P. 1986, *A&A*, 164, 86
- Petrenz, P., & Puls, J. 2000, *A&A*, 358, 956
- Poe, C. H., Owocki, S. P., & Castor, J. I. 1990, *ApJ*, 358, 199
- Porter, J. M., & Drew, J. E. 1995, *A&A*, 296, 761
- Porter, J. M., & Skouza, B. A. 1999, *A&A*, 344, 205
- Puls, J., Springmann, U., & Lennon, M. 2000, *A&AS*, 141, 23
- Scuderi, S., Panagia, N., Stanghellini, C., Trigilio, C., & Umana, G. 1998, *A&A*, 332, 251
- Springmann, U. W. E., & Pauldrach, A. W. A. 1992, *A&A*, 262, 515
- Vink, J. S., De Koter, A., & Lamers, H. J. G. L. M. 1999, *A&A*, 350, 181
- Vink, J. S., De Koter, A., & Lamers, H. J. G. L. M. 2000, *A&A*, 362, 295
- Waters, L. B. F. M., Marlborough, J. M., Geballe, T. R., Oosterbroek, T., & Zaal, P. 1993, *A&A*, 272, L9
- Zaal, P. A., de Koter, A., Waters, L. B. F. M., et al. 1999, *A&A*, 349, 573